

- 305 (1966).
5. Douglas, J. M., and N. Y. Gaitone, *Ind. Chem. Fundamentals*, **6**, 265 (1967).
 6. Gaitonde, N. Y., and J. M. Douglas, *AIChE J.*, **15**, No. 6, p. 902 (Nov., 1969).
 7. Gilles, E. D., "Grundloggen der Chemischen Progress-regelung," W. Oppelt and E. Wicke, ed., R. Oldenbourg Verlag, Munchen-Wien, Germany (1964).
 8. Hoffman, H., "Proceedings of the Third European Symposium on Chemical Reaction Engineering," p. 283, Pergamon Press, London, England (1965).
 9. Kermode, R. I., and W. F. Stevens, *Can. J. Chem. Eng.*, **43**, No. 2, 68 (1965).
 10. Luus, R., and L. Lapidus, *Chem. Eng. Sci.*, **21**, 159 (1966).
 11. Simpkins, R. C., and D. E. Lamb, *Proc. IACL*, 486 (June, 1963).
 12. Swain, C. G., and C. B. Scott, *J. Am. Chem. Soc.*, **75**, 246 (1953).
 13. Tinkler, J. D., and D. E. Lamb, *Chem. Eng. Progr. Symposium Ser.*, No. 55, **61**, 155 (1965).
 14. Wu, D., Sc.D. thesis, Mass. Inst. Technol., (1962).
 15. Zimmerman, G., and C. Yuan, *J. Am. Chem.*, **77**, 332 (1955).

Manuscript received April 18, 1968; revision received August 7, 1968; paper accepted August 9, 1968.

APPENDIX: TERMS IN ANALYTICAL SOLUTION

Transformation Matrix

$$P = \begin{pmatrix} P_{11} & P_{12} \\ P_{21} & P_{22} \end{pmatrix} = \begin{pmatrix} 2\alpha_0 + 2[1 + \beta_1(2 + \beta_0)] & 2\omega_0 \\ -2\beta_5(2 + \beta_0) & 0 \end{pmatrix}$$

Constants in Solution

$$K_1 = -2\beta_3\beta_5 \{3[1 + \alpha_0 + \beta_1(2 + \beta_0)]^2 + \omega_0^2\} \\ - 3\beta_3\beta_5^2(2 + \beta_0)^2(2 - \beta_3)[1 + \alpha_0 + \beta_1(2 + \beta_0)]$$

$$K_2 = -4\beta_1\beta_3\beta_5(2 + \beta_0)[1 + \alpha_0\beta_1(2 + \beta_0)] \\ - \beta_1\beta_3\beta_5^2(2 + \beta_0)^3(2 - \beta_3)$$

$$K_3 = \beta_3\beta_5[1 + \alpha_0 + \beta_1(2 + \beta_0)] \\ \{4[1 + \alpha_0 + \beta_1(2 + \beta_0)] + \beta_5(2 + \beta_0)^2(2 - \beta_3)\}$$

$$K_4 = -\beta_3\beta_5\omega_0 \{4[1 + \alpha_0 + \beta_1(2 + \beta_0)] \\ + \beta_5(2 + \beta_0)^2(2 - \beta_3)\}$$

$$K_5 = [2\beta_1\beta_3\beta_5(2 + \beta_0)/\omega_0] \{3[1 + \alpha_0 + \beta_1 \\ (2 + \beta_0)]^2 + \omega_0^2 + 3\beta_5(2 + \beta_0)^3 \cdot \\ (2 - \beta_3)[1 + \alpha_0 + \beta_1(2 + \beta_0)]\}$$

$$K_6 = -(\beta_3\beta_5/\omega_0)[1 + \alpha_0 + \beta_1(2 + \beta_0)] \\ \{6[1 + \alpha_0 + \beta_1(2 + \beta_0)]^2 + \omega_0^2 \\ + 3\beta_5^2\beta_3(2 + \beta_0)^2[1 + \alpha_0 + \beta_1(2 + \beta_0)]\}$$

$$K_7 = (\beta_1/\omega_0) \{[1 + \alpha_0 + \beta_1(2 + \beta_0)]^2 + \omega_0^2\} \\ + (\beta_1\beta_3\beta_5^2/2\omega_0)(1 + \beta_0)(2 + \beta_0)^2(\beta_3 - 2) \\ - (\beta_1\beta_3\beta_5/\omega_0)(2 + \beta_0)^2[1 + \alpha_0 + \beta_1(2 + \beta_0)]$$

$$K_8 = \{[1 + \alpha_0 + \beta_1(2 + \beta_0)]/2\omega_0(2 + \beta_0)\} \\ \{2\beta_3\beta_5(2 + \beta_0)^2[1 + \alpha_0 + \beta_1(2 + \beta_0)] - 2\omega_0^2 \\ - 2[1 + \alpha_0 + \beta_1(2 + \beta_0)]^2 \\ - \beta_3\beta_5^2(2 + \beta_0)^2(1 + \beta_0)(\beta_3 - 2)\}$$

$$K_9 = [1/2(2 + \beta_0)] \{2\beta_3\beta_5(2 + \beta_0)^2 \\ [1 + \alpha_0 + \beta_1(2 + \beta_0)] - 2\omega_0^2 \\ - 2[1 + \alpha_0 + \beta_1(2 + \beta_0)]^2 \\ - \beta_3\beta_5^2(2 + \beta_0)^2(1 + \beta_0)(\beta_3 - 2)\}$$

Single Drop Breakup in Developing Turbulent Pipe Flow

JOHN E. SWARTZ and DAVID P. KESSLER

Purdue University, West Lafayette, Indiana

An experimental study was made on the breakup of a single drop in two phase liquid-liquid developing turbulent pipe flow. The predominant breakup mechanism was controlled by dynamic pressure forces, and the drop breakup was characterized by one or two smaller drops breaking off a larger drop.

The effect on the increase in interfacial area and the resulting size distribution of the fragmented drops of drop velocity, interfacial tension, initial drop size, and the distance down the pipe was studied. Regression analysis was used to determine the significant effects. Most of these regression equations had significant cubic and two-factor interactions, which is indicative of the complexity of drop breakup.

The size distribution of the fragmented drops can be approximated by a normal distribution. However, the steady state distribution was not fully developed in the work here.

In many two phase liquid-liquid operations in chemical engineering, where mass is being transferred between

phases, the mass transfer step is the rate determining step in the operation. The mass transfer of species A depends upon the mass transfer coefficient, the interfacial area, and the chemical potential of A in each of the two phases,

John E. Swartz is with Monsanto Company, Alvin, Texas.

that is, the driving force between the phases. If we assume the concentration of A in the continuous phase to be constant, the mass transfer driving force is directly proportional to the concentration of A in the individual drops of the dispersed phase.

For a population of different size drops at the same initial concentration, the mass transfer rate and hence the concentration of A will behave differently in time for different drop sizes; for example, in smaller drops, which have a larger surface area per unit mass, the concentration of A will initially decrease faster and at any time will be less than in a larger drop. If each drop remained intact, after a period of time most of the mass transfer would be between the continuous phase and the relatively less depleted larger drops.

However, drops are continuously losing identity through coalescence and fragmentation. In a sufficiently mixed system, the drops with a lower concentration of A may coalesce with other drops with a high concentration of A, and the resulting drops may then be fragmented into smaller drops of essentially equal concentrations of A. However, there is very little information available on just how the concentration distributions and the size distributions of drops are changing, although a theory based on population balance methods is developing. There is a great need for experimental investigations along these lines.

As an approach to part of the problem, this investigation is an experimental study of the breakup of a single drop in two phase liquid-liquid developing turbulent pipe flow. The drop was broken up by the exclusive action of the forces present in the developing turbulent flow of a continuous phase in a straight circular glass pipe. Specifically studied were the effects of drop velocity, interfacial tension, initial drop size, and the distance down the pipe upon increase in interfacial area and the resulting size distribution of the fragmented drops.

DISCUSSION

Drops in a turbulent flow field are subject to a variety of forces: buoyancy, gravity, drag or external viscous forces, inertial or dynamic pressure forces from velocity fluctuations, surface forces, and internal viscous forces. If the deformation resulting from these forces is too large, the drop becomes unstable and breaks up.

The most important of these forces for relatively low viscosity liquid pairs and turbulent flow are the inertial forces, the surface forces, and the pressure forces. The effects of these forces can be studied in developing turbulent flow in terms of the following dimensionless groups: $(DV\rho_c)/(\mu_c)$, the Reynolds number; $(DV^2\rho_c)/(\sigma)$, the Weber number; $(\rho_d)/(\rho_c)$, $(\mu_d)/(\mu_c)$, and L/D . Note that both the Reynolds number and the Weber number are based on the pipe diameter, since this is common practice, although the drop diameter must have some effect.

The experimental work was designed to study the effects of the more significant dimensionless groups describing breakup of a single drop. These effects were studied for drops of different initial diameters. In this investigation, the densities and viscosities of the two phases remained essentially constant, so these variables were not studied.

Other investigators (2, 6) have shown that the Weber number has a much greater effect on drop breakup than the Reynolds number. Also, the more significant of the two forces in the Reynolds number under turbulent flow, inertial force, is also present in the Weber number. Because of these observations, the effect of the Reynolds number was not studied. Therefore, the relationship among the dimensionless groups was reduced to the following form:

Y = f(N_{We} , L/D)

By including various initial conditions (the initial drop diameter) in the effects studied, and by removing D (a constant) from the L/D term for simplicity, the following relationship was the form investigated:

$$Y = g(N_{We}, d_0, L_t)$$

To investigate these variables, a three-factor factorial experiment was designed as shown in Figure 1. A total of seventeen treatments were run, each treatment or cell having from five to ten replicates.

The Weber number was studied over a range as large as possible within the limitations of the equipment; Weber number values were 1,160, 1,410, 1,840, 2,180, and 2,840. The initial drop sizes and the distance down the pipe were run at two levels each. The initial drop sizes were 1.2 and 1.5 cm., and the distances the drops traveled down the pipe were 20 and 35 ft. A summary of experimental conditions is given in Table 1. For runs 1 through 9, the initial drop diameter was 1.2 cm. and for runs 10 through 17, 1.5 cm. Runs 1 to 4 and 10 to 14 were for $L = 20$ ft.; others are for $L = 35$ ft.

EQUIPMENT

The equipment consisted of a recirculating system containing two liquid reservoirs, centrifugal pump, electric solenoid valve, injection tee, glass pipe, and return piping as shown in Figure 2.

The liquid reservoirs were two 55-gal. drums coated internally with a polymeric material. A Worthington model 1DN62 centrifugal pump was used to recirculate the water. A $\frac{1}{2}$ in. electric solenoid valve was used for quickly starting and stopping the flow. The liquid velocity was controlled with a $1\frac{1}{2}$ in. globe valve.

The injection tee was a $1\frac{1}{2}$ in. \times $1\frac{1}{2}$ in. \times $\frac{1}{2}$ in. glass tee as shown in Figure 3. An 18-gauge hypodermic needle was inserted into the leg of this tee to enable the liquid drop to be transferred from a hypodermic syringe to the interior of the pipe.

The pipe consisted of four 10-ft. sections of $1\frac{1}{2}$ in. tempered glass pipe. The inside diameter was 1.50 ± 0.01 in. The neoprene gaskets between the glass joints were 1.56 in. I.D. When the glass pipe was assembled, careful attention was given so that each section was in axial alignment and was horizontal. Standard galvanized pipe and fittings were used between the reservoirs and the flow regulating valve. From this valve $1\frac{1}{2}$ in. PVC plastic pipe and fittings were used to the injection tee and as a return line from the glass pipe to the reservoirs.

All wetted parts were cleaned with a solvent and dried before assembly. The system was operated with numerous changes of water before data were taken.

EXPERIMENTAL PROCEDURE

Ordinary city water was used as the continuous phase. No runs were made for at least 24 hr. after the water was changed to allow the system to come to room temperature. Two different mixtures were used as the dispersed phase in order to vary the interfacial tension while keeping the densities and viscosities relatively constant. System A was a mixture of isooctane and carbon tetrachloride; system B was a mixture of benzene and nitrobenzene. The dispersed phase was dyed with a small amount of Oil Red dye for visibility.

The two phases were always mutually saturated before data were taken. The continuous phase was saturated by adding a small amount of this dispersed phase to the reservoirs and by circulating the system for at least 30 min. For the dispersed phase, a small amount of water was poured into the reagent bottle and the phases mixed.

System

Run No.	Replications	System	V	c	Average number of drops	Mean diameter	Percent increase in surface area	Reduced mean diameter	d_p/d_o
1	8	A	128	44	2.9	0.62	10.7	0.33	0.96
2	5	A	146	44	5.6	0.49	32.8	0.36	0.91
3	5	B	128	28.5	12.0	0.38	70.4	0.33	0.82
4	5	B	146	28.5	26.8	0.28	113.5	0.26	0.74
5	5	A	115	44	2.6	0.66	12.3	0.36	0.96
6	10	A	128	44	4.4	0.58	31.3	0.43	0.90
7	5	A	146	44	12.2	0.40	78.2	0.36	0.79
8	5	B	128	28.5	21.6	0.32	112.5	0.29	0.71
9	5	B	146	28.5	75.6	0.23	241.6	0.22	0.51
10	10	A	128	44	3.4	0.70	11.7	0.39	0.96
11	5	A	146	44	10.0	0.46	51.2	0.37	0.86
12	5	B	128	28.5	19.6	0.39	90.2	0.35	0.77
13	5	B	146	28.5	50.4	0.28	161.2	0.27	0.61
14	10	A	128	44	7.0	0.56	42.3	0.44	0.88
15	7	A	146	44	19.0	0.40	93.0	0.36	0.77
16	6	B	128	28.5	48.2	0.30	170.6	0.29	0.60
17	5	B	146	28.5	107.8	0.25	268.0	0.24	0.51

Drops with diameters smaller than 0.1 cm. were not included, primarily because of the difficulty of measuring these small drops directly in the pipe. These drops represented 10 to 20% of the total number of drops. Even if 20% more drops had diameters of 0.09 cm., the surface area of the fragmented drops would be increased only 2 to 3%. Thus, these drops have a negligible effect upon the volume and surface area of the fragmented drops.

All measurements on the dispersed phase were made after the addition of the dye. The liquid viscosities and densities are accurate within approximately 5%. They

The accuracy of the observed drop diameters after breakup was determined by computing the total volume of the dispersed drops for each run and comparing this against the volume of the initial drop. This comparison is shown in Table 2. Fifty-three observations were made at

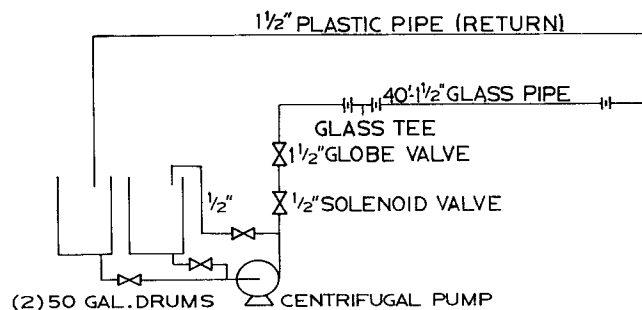


Fig. 2. Experimental equipment.

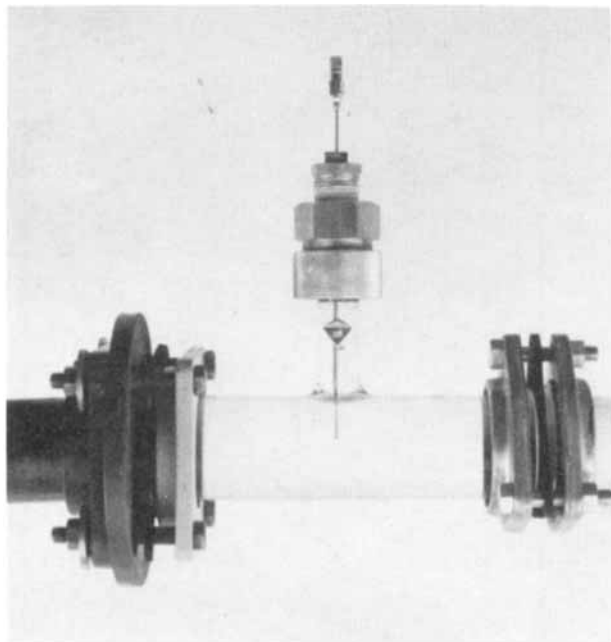


Fig. 3. View of injection tee.

each of the initial drop diameters.

The difference is caused primarily by parallax when the drop diameter is measured in the pipe; however, this bias introduces an error of only 3 and 5% in the volumes of the 1.2 and 1.5 cm. drop diameters, respectively, and less error in the surface areas and drop diameters.

Replicates 1 to 5 of run 14 were some of the earliest made. To detect any change in the accuracy and precision of the experimental procedure, replicates 6 to 10 of run

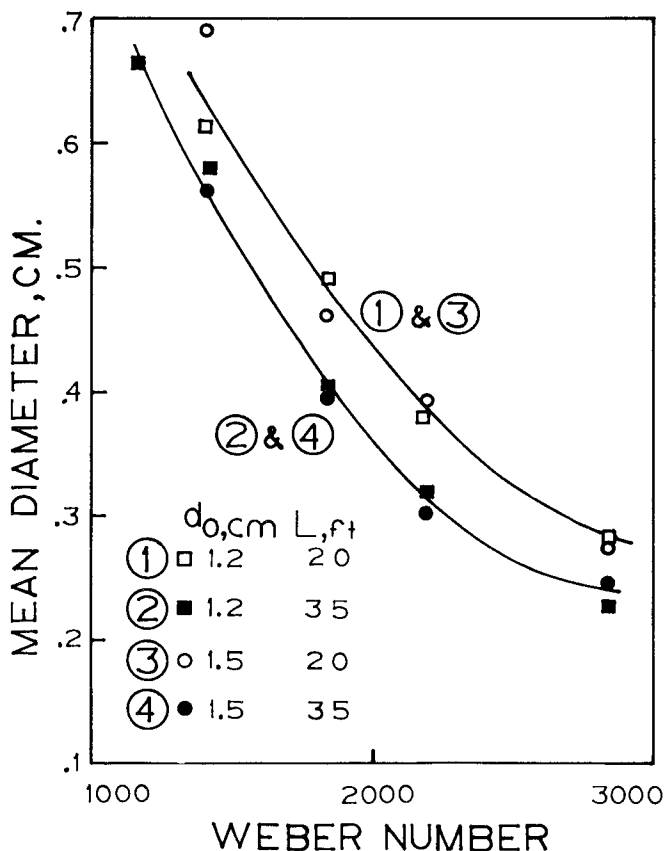


Fig. 5. Effect of Weber number on the mean diameter of fragmented drops.

14 were the last data determined. Statistical tests give no evidence that the means and variances of these two sets of replicates are different.

RESULTS

Observations of the Fragmentation Process

The dyed drops were easily observed as they moved down the glass pipe. Upon start-up of the continuous phase, the drop moved down the pipe and started vibrating. These vibrations were of the type described by Hinze (1) as the penetration of lamellae and ligaments of one fluid into the other. Almost all of the breakups were characterized by one or two smaller drops breaking from the large parent drop rather than the parent drop splitting into two more or less equal size drops or a drop shattering, where four or five smaller drops were simultaneously formed from the larger drop.

Throughout the drop acceleration and initial stages of breakup, the drop remained near the center of the pipe, and the breakup also occurred near the center. In similar experimental equipment in developed flow, Sleicher (4) observed that most of the drop breakup occurred very close to the wall, and that each drop broke into two approximately equal parts after considerable stretching.

As a drop accelerates in turbulent flow, the decrease in pressure on one side caused by higher velocities of the continuous phase will tend to pull the drop into the center of the pipe. As the drop approaches the velocity of the continuous phase, the greatest velocity differential across the drop occurs on that side closer to the wall. This velocity differential will lower the pressure on the side nearer the wall and cause the drop to move towards the wall. As the drop moves into lower velocity fields, it slows down;

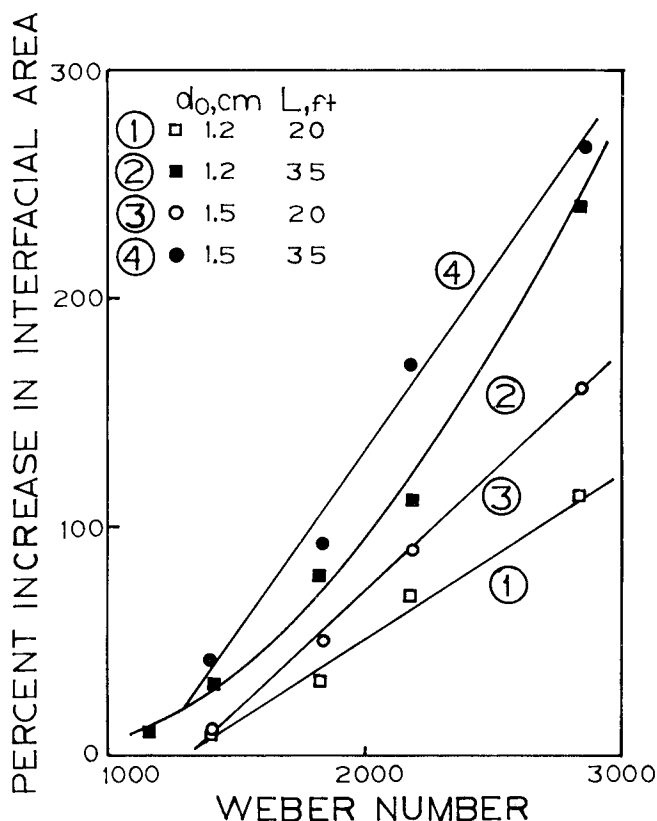


Fig. 4. Effect of Weber number on interfacial area.

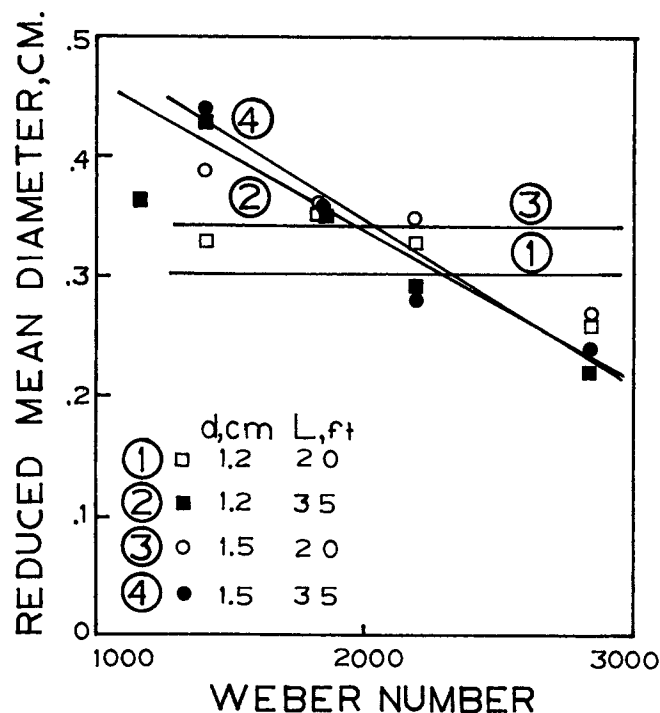


Fig. 6. Effect of Weber number on the reduced mean diameter of fragmented drops.

that portion near the wall decelerates faster creating shear forces on the drop. These forces are acting simultaneously with the random pressure fluctuations of turbulent flow.

It is generally acknowledged that there seem to be two predominant mechanisms for drop breakup depending upon whether the drop breaks up near the wall (shear forces) or near the center of the pipe (pressure forces). The shear forces stretch the drop and split it into approximately equal parts, and the pressure forces cause the drops to vibrate with smaller drops breaking off.

The distance a drop was exposed to turbulent flow varied somewhat from replicate to replicate, even though the total distance traveled was the same. That is, for a duplicate run, the drop was initially subjected to turbulent stresses at varying distances from the injection tee because there was some uncontrollable variation in the speed at which turbulence developed.

To determine where the transition from laminar to turbulent flow took place, lines of dye were injected into the water perpendicular to the pipe axis in the proximity of the drop. A run was made exactly as if data were being taken. As long as the flow was laminar, the dye lines retained their identity; when turbulent flow started, the dye lines quickly mixed with the continuous phase and lost their identity. This test was repeated a number of times, and each time the drop remained almost spherical in shape during laminar flow but immediately started vibrating with bulgy deformations at the onset of turbulent flow. Therefore, in subsequent runs, the initiation of turbulent flow was taken as the point where the drop started vibrating.

The initiation of turbulent flow varied about a mean distance of approximately 13 ft. from the injection tee. This is comparable to Sleicher's data (4). He states that 11 ft. are required for the development of the boundary layer. It is believed that some of this variation was caused by the slightly irregular action of the solenoid valve.

No drops were observed to be fragmented during the acceleration and deceleration of the flow. After the drop had reached a given distance, the solenoid switch was closed, and the drop made a sudden stop approximately

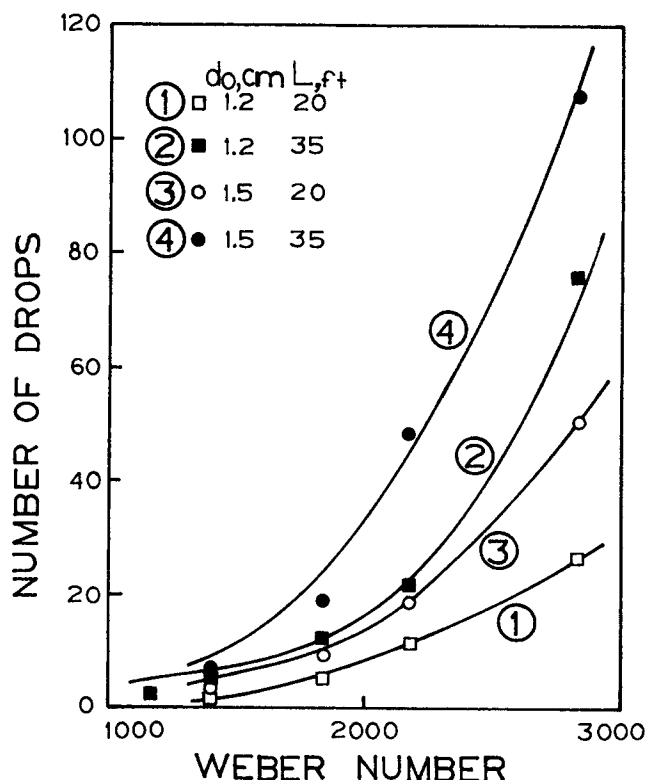


Fig. 7. Effect of Weber number on the number of fragmented drops.

3 ft. further downstream (less than 1 sec.).

No observations were made of any drops coalescing during a run. Indeed, one would not expect any coalescence with such a small amount of dispersed phase present. The latter two observations also agree with Sleicher (4).

Correlation of Data

A number of dependent variables were used to display the results of this investigation. These results are shown on Figures 4, 5, 6, 7, and 8, where the dependent variables are increase in interfacial area, mean diameter of

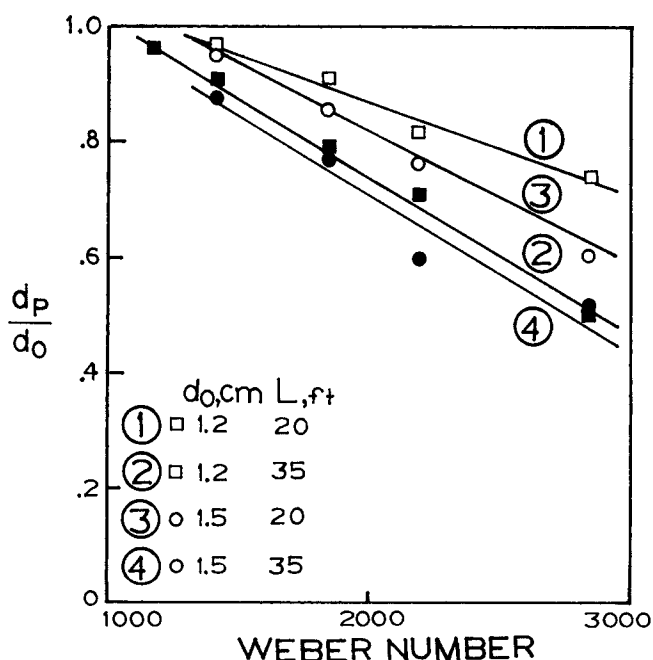


Fig. 8. Effect of Weber number on the parent drop size.

the fragmented drops, reduced mean diameter (with the largest, that is, parent, drop removed), the number of fragmented drops n , and the parent drop diameter divided by the initial drop diameter d_p/d_0 . The curve parameters are the initial drop size and the distance the drop traveled down the pipe.

The average value of these dependent variables for each run are tabulated in Table 1 and are the data points shown on Figures 4 to 8. Each data point shown on these curves represents the average response for one treatment or cell of the experiment. All the curves on Figures 4, 6, 7, and 8 were determined by a regression analysis by using the general multiple regression program BIMD 3R on an IBM 7094 computer. The curves on Figure 5 were not determined in this manner.

The regression model for these curves is a specific case of the general model given below with d_0 and L_t terms held constant:

$$Y = b_0 + b_1 (N_{we}) + b_2 (N_{we})^2$$

There was no significant lack of fit in any of these curves at $\alpha = 0.10$.

Analytical equations were also developed for these effects by using all three independent variables studied. The following model was used:

$$Y = b_0 + b_1 (N_{we}) + b_2 (N_{we})^2 + b_3 (N_{we})^3 + b_4 (d_0) + b_5 (L_t) + b_6 (N_{we}) (d_0) + b_7 (N_{we}) (L_t) + b_8 (d_0) (L_t) + b_9 (N_{we}) (d_0) (L_t)$$

The significant terms in this model were determined for each dependent variable with a regression analysis by using the BIMD 3R program and an IBM 7094 computer. To obtain no significant lack of fit at $\alpha = 0.10$, all terms had to be included for $Y = n$. For $Y = I$, all terms except the ones involving b_5 , b_8 , and b_9 had to be included. For $Y = X_r$, only terms in b_0 , b_1 , b_5 , and b_7 were included. For $Y = d_p/d_0$, only terms in b_8 and b_9 were excluded.

Discussion of Results

With reference to Figure 4, the regression curves 1, 3, and 4 are linear, while curve 2 is quadratic. However, curve 2 has five levels of observations, while the other curves have only four levels. One might expect all the curves in Figure 4 to approach quadratic curves if the range of the observations was increased.

In Figure 6, curves 1 and 3 are horizontal, indicating that there are no significant differences in the reduced drop diameters within the range of Weber numbers investigated. Curves 2 and 4 are linear with negative slopes. However,

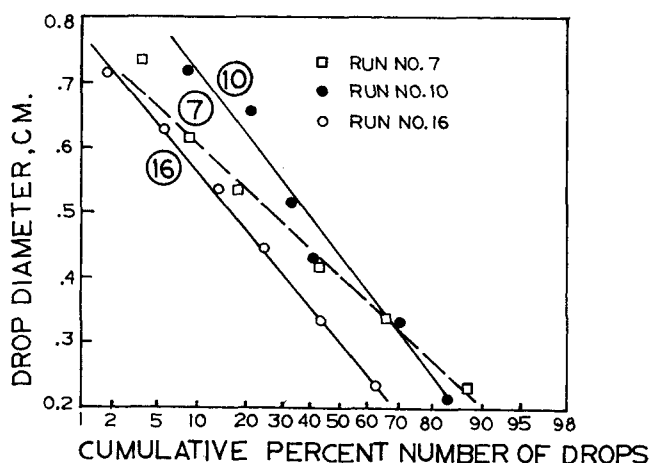


Fig. 9. Cumulative distributions of drop diameters.

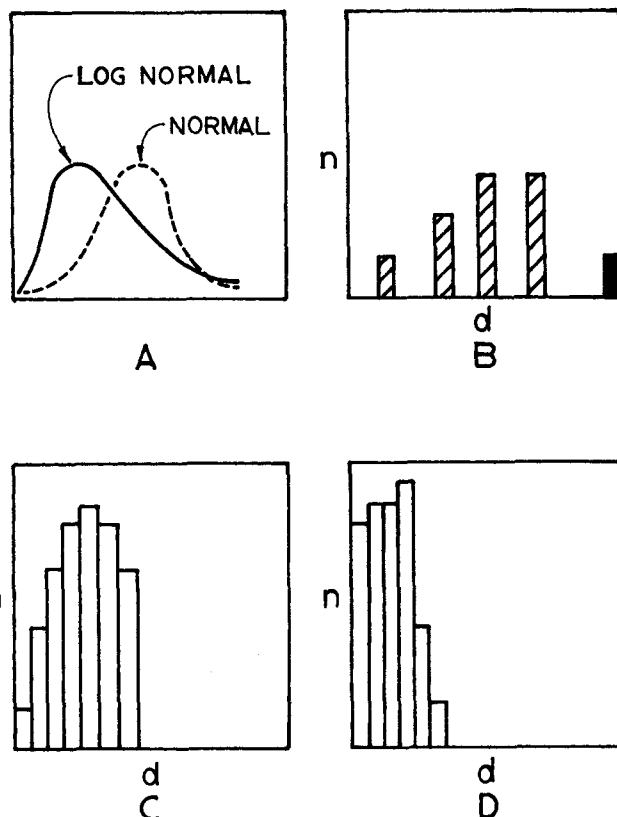


Fig. 10. Evolution of drop size distribution.

in curves 1 and 3 the total distance the drop traveled in the pipe was only 20 ft.; thus, the drop breakup was not sufficient to detect any differences in reduced mean drop diameters. In curves 2 and 4, the total distance the drop traveled was 35 ft., and differences in the reduced mean drop diameters could be detected. These results are what one might expect in developing flow.

Examination of the regression equations shows a large number of the independent variables (N_{we} , d_0 , and L_t) and their interactions to be significant, even though two independent variables were measured at only two levels within a short range. For example, the regression equation for the increase in interfacial area has the following significant terms:

$$I = b_0 + b_1 (N_{we}) + b_2 (d_0) + b_3 (L_t) + b_{11} (N_{we})^2 + b_{111} (N_{we})^3 + b_{12} (N_{we}) (d_0) + b_{13} (N_{we}) (L_t)$$

This suggests that the increase in interfacial area is dependent upon many variables and their interactions and is a very complicated expression. If the effect of other important factors such as viscosity and density were studied, these expressions would be even more complicated.

The authors know of no other data that would invite comparisons with this investigation. The closest work is

TABLE 2. COMPARISON OF DROP VOLUMES

	Initial drop 1.2	Diameter, cm. 1.5
Initial volume, cc.	0.9048	1.767
Mean of the final volumes, cc.	0.8748	1.681
Standard error of the final volumes	0.0259	0.040

the numerous papers (2, 3, 7) on liquid jets mixing two phases. In most of these a liquid jet of the dispersed phase was injected into a flowing continuous phase and the resultant drops analyzed. After the jet had initially broken up to form drops, further breakup would probably be of the type discussed in this investigation. Once the individual drops are formed, subsequent breakup is not, of course, dependent on the origin of the drops.

Examination of the raw data shows that the fragmentation process was nowhere near completion when each run was terminated. In almost every observation the resulting drops consisted of a large parent drop with a number of much smaller drops. In Figures 5 and 6, at a Weber number greater than approximately 3,000, the mean drop diameters of the two populations (total and reduced) blend into the same curves. This suggests that at these Weber numbers the parent (or largest remaining) drop was sufficiently fragmented to have little effect on the mean diameter of the fragmented drops.

Drop Size Distribution

The cumulative distributions of the diameters of the fragmented drops (exclusive of the parent or largest remaining drop) for runs 7, 10, and 16 were plotted on probability paper. All of these runs approximated a straight line, indicating a close fit to a normal distribution for the fragmented drop diameters. These plots are given in Figure 9. Other investigators (2, 6) have found that dispersed drop diameters follow a log-normal distribution. However, their systems were different than the one studied in this investigation in that their dispersed phase was continuously entering the system in the form of a liquid jet. A log-normal distribution is characterized by a larger percentage of drops at the smaller diameters as shown in Figure 10A.

In this investigation, the initial drop size distribution was a single drop as shown by the solid area in Figure 10B. After the drop had fragmented approximately eight or nine times, the size distribution would be similar to that shown by the shaded areas in Figure 10B. As the drops continued to break up, one would expect the size distribution to be similar to a truncated normal distribution as shown in Figure 10C, where the distribution is bounded by zero on one side and the largest drop diameter (which, of course, must be less than the initial drop diameter) on the other side.

If breakup were continued beyond the range of this investigation, one might expect the distribution of drop diameters to approach that shown in Figure 10D, where the entire population would be in a narrow diameter range. This final distribution (beyond which no further breakup will occur) might be expected to approach a truncated log-normal distribution because of this high population density in the smaller diameters. Thus, this investigation is not inconsistent with the finding of log-normal drop distributions by other investigators.

CONCLUSIONS

1. Analytical equations were found for different dependent variables by using the Weber number, initial drop size, and distance traveled in turbulent flow as the dependent variables. A number of terms involving two- and three-factor interactions is required in some of these equations to obtain significant fit of the data. Because of the large number of terms and interactions, caution must be used in attempting to use these equations beyond the range of the data.

2. The regression equation for the percent increase in interfacial area is

$$I = 741.8 - 1.06 (N_{We}) + 4.81 \times 10^{-4} (N_{We})^2 \\ - 7.48 \times 10^{-8} (N_{We})^3 - 137.7 (d_0) - 2.66 (L_t) \\ + 1.07 \times 10^{-1} (N_{We}) (d_0) \\ + 3.02 \times 10^{-3} (N_{We}) (L_t)$$

3. The predominant breakup mechanism was by pressure forces. The drop breakup was characterized by one or two smaller drops breaking from a large drop.

4. The size distribution of the fragmented drops can be approximated by a normal distribution. However, because the breakup was terminated in the early stages, this is not inconsistent with the log-normal distribution found by other investigators.

5. During the earlier stages of breakup, the number of drops formed with diameters of less than 0.1 cm. is approximately 10 to 20% of the total number of drops, and their contribution to the total interfacial area is insignificant. However, as breakup continues, one might expect the relative number of these smaller drops to increase.

NOTATION

b_i	= constants in regression models
d_0	= initial drop diameter, cm.
d_p	= parent (or largest remaining) drop diameter, cm.
D	= pipe diameter, cm.
I	= percent increase in interfacial area
L	= total distance drop has traveled from rest, ft.
L_t	= total distance drop has traveled in turbulent flow, ft.
n	= number of drops
N_{Re}	= Reynolds number, dimensionless
N_{We}	= Weber number, dimensionless
s_r	= standard deviation about the reduced mean
V	= average bulk velocity, cm./sec.
X_i	= independent variables in regression models
X_r	= reduced mean drop diameter, cm.
X_t	= arithmetic mean drop diameter, cm.
Y	= dependent variable in regression model

Greek Letters

α	= probability associated with the F value in statistical tests
μ_c	= viscosity of continuous phase, centipoise
μ_d	= viscosity of dispersed phase, centipoise
ρ_c	= density of continuous phase, g./cc.
ρ_d	= density of dispersed phase, g./cc.
σ	= interfacial tension, dynes/cm.

LITERATURE CITED

1. Hinze, J. O., *AIChE J.*, 1, No. 3 (Sept., 1955).
2. Roy, Paul H., Ph.D. thesis, Ill. Inst. Technol., Chicago (1955).
3. Shinnar, Reuel, *J. Fluid Mech.*, 10, 259 (1961).
4. Sleicher, C. A., Jr., *AIChE J.*, 8, No. 4 (Sept., 1962).
5. Paul, H. I., and C. A. Sleicher, Jr., *Chem. Eng. Sci.*, 20, 57-9 (1965).
6. Kessie, R. W., MS thesis, Ill. Inst. Technol., Chicago (1955).
7. Baranayev, M. K., Ye. N. Teveroskiy, and E. L. Tregubova, *Dokl. Akad. Nauk SSSR*, 66, 821 (1949).
8. Hinze, J. O., "Turbulence," McGraw-Hill, New York (1959).
9. Zuidema, H. H., and G. W. Waters, *Ind. Eng. Chem. Anal. Ed.*, 13, 312 (1941).
10. Swartz, J. E., MS thesis, Purdue Univ., West Lafayette, Ind. (1967).

Manuscript received March 31, 1967; revision received July 16, 1968
paper accepted August 12, 1968.